MULTI-LINEAR-ELEMENT DEPTH-INTEGRATED MODELS FOR FLOWS WITH A FREE SURFACE

Zhengtong Yang, Technology Centre for Offshore and Marine, Singapore (TCOMS), yang_zhengtong@tcoms.sg
Philip L.-F. Liu, National University of Singapore, philip.liu@nus.edu.sg

INTRODUCTION
In this study, we derive a new set of depth-integrated models for solving unsteady flows that satisfy the Euler equations and nonlinear free surface boundary conditions in the σ-coordinates. One of the obvious differences between the present approach and the ones directly solving the 3D Euler equations using Finite Element Method (FEM) is that in the present model the vertical velocity and the pressure field are eliminated by integrating the continuity equation and vertical momentum equation, respectively. Therefore, the present models only solve the horizontal velocity components and the free surface displacement in the two-dimensional horizontal (2DH) space. The new models are also more advantageous in using fewer elements in the vertical direction while achieving better performance. At this stage, the capability and application of the new models in dealing with free surface wave propagation problems are addressed.

MATHEMATICAL MODELS
For models derived in Yang & Liu (2020) the basic assumption is that one polynomial of a certain degree is used to approximate the horizontal velocity profile in the entire water column, yielding models of different complexity and accuracy. In this study, following the concept of FEM, instead of using one polynomial to approximate the vertical profile of horizontal velocity in the entire water column, the total water depth is divided into several elements, and the horizontal velocity profile within each element is approximated by a linear function in terms of the vertical coordinate. The continuity of velocity and pressure fields at the interface between elements are then enforced. And the resulting residuals from the horizontal momentum equations are minimized via the method of weighted residuals. Finally, a set of 2DH governing equations is derived. The complexity and accuracy of the final resulting models strongly depend on the number of elements as well as the elevations of the element interfaces.

For demonstration purposes, we show explicitly the model equations of a two-linear-element model, i.e. *ME-2L* in 1DH space. For brevity, only linear terms in the governing equations on a constant water depth (i.e., $h(x) = d$ are shown here, i.e., the depth-integrated continuity equation

$$\frac{\partial \eta}{\partial t} + \frac{1}{2}d\left[c_2\frac{\partial u_1}{\partial x} + \frac{\partial u_2}{\partial x} + (1-c_2)\frac{\partial u_3}{\partial x}\right] + N.L. = 0, \qquad (1)$$

and three momentum equations which are written in a matrix form for better clarity,

$$\begin{pmatrix} A_{11} & A_{12} & A_{13} \\ A_{21} & A_{22} & A_{23} \\ A_{31} & A_{32} & A_{33} \end{pmatrix}\begin{pmatrix} \frac{\partial u_1}{\partial t} \\ \frac{\partial u_2}{\partial t} \\ \frac{\partial u_3}{\partial t} \end{pmatrix} + \begin{pmatrix} B_{11} & B_{12} & B_{13} \\ B_{21} & B_{22} & B_{23} \\ B_{31} & B_{32} & B_{33} \end{pmatrix}\begin{pmatrix} d^2\frac{\partial^3 u_1}{\partial x^2 \partial t} \\ d^2\frac{\partial^3 u_2}{\partial x^2 \partial t} \\ d^2\frac{\partial^3 u_3}{\partial x^2 \partial t} \end{pmatrix} + \begin{pmatrix} 3 \\ \frac{3}{2} \\ 3 \end{pmatrix}g\frac{\partial \eta}{\partial x} + \begin{pmatrix} N.L. \\ N.L. \\ N.L. \end{pmatrix} = \begin{pmatrix} 0 \\ 0 \\ 0 \end{pmatrix}$$

$$(2)$$

where η is the free surface elevation; u_1, u_2, u_3 are the horizontal velocities located at the bottom, interface between two elements, i.e., $\sigma = c_1$, and free surface, respectively. Additionally, *A* and *B* are various coefficients which are functions of c_1 and *N.L.* denotes all the nonlinear terms in the full expressions. It should be noted that the highest spatial derivative always remains at three regardless the number of elements.

Compared with direct FEM for solving the Euler equations, in the present formulation, the discretization in the vertical direction by using linear elements is analytically incorporated into derivations, resulting in governing equations that can be solved by various numerical methods in 2DH space. On the other hand, the present model can be considered as a multi-element extension of the *G2* model developed in Yang & Liu (2020), in which shape functions are used for weighting functions. Whereas the *G2* model assumes a linear profile on the horizontal velocity in the entire water column, the present models employ multiple linear profiles matched at the element interface to describe the horizontal velocity profile. And the elevations of interfaces between elements are free parameters that can be tuned for different modelling purposes.

THEROTICAL ANALYSIS
A Stokes wave-type Fourier analysis is conducted on the new models up to four linear elements to examine their linear wave properties, including linear wave phase velocity, group velocity and shoaling gradient. Firstly, after an optimization on the free parameter, the performance of the *ME-2L* model, in which the total water depth is divided into two elements, is compared with other two-layer models, which include the two-layer Boussinesq model (Lynett & Liu 2004) and the two-equidistant-layer non-hydrostatic SWASH model (Stelling & Zijlema 2003). However, it should be noted that the number of horizontal velocity unknowns of both the two-layer Boussinesq model and the two-equidistant-layer non-hydrostatic SWASH model is two. The Galerkin model (*G3*) and subdomain model (*S3*) developed in Yang & Liu (2020) are also included for comparison in the following discussions since both models contain three horizontal velocity unknowns, which is the same as the *ME-2L* model.

The comparisons of various linear wave properties in terms of phase velocity, group velocity, shoaling gradient, and integrated shoaling gradient among above-mentioned models are displayed in figure 1. Generally,

these models show similar accuracy in terms of the linear wave phase velocity which are applicable up to $kd \approx 7$. However, a detailed inspection shows that the *G3* model deviates from the exact solution the earliest, followed by the two-layer Boussinesq model, two-layer SWASH model, *S3* model, and *ME-2L* model, for increasing kd values. It can be observed that while the rest of the models are accurate in relatively shallow water up to $kd \approx 7$, the two-layer SWASH models show small undulations locally around $kd < 2$. The comparisons of group velocity, shoaling gradient, and integrated shoaling gradient are also shown in figure 1(b), (c), and (d), respectively. Similar to the behavior of linear phase velocity, the *ME-2L* model outperforms the other four models in both characteristics. These models also share the same feature that the applicable ranges of the model in terms of group velocity and shoaling gradient are smaller than those in terms of phase velocity. Finally, by specifying an error bound of 2%, we find the *ME-2L* model can be applied up to $kd = 14.7$ in terms of phase velocity, which is essentially in very deep water and larger than the other four models. The applicable range of kd values for the *ME-2L* model is also more than twice to that of the *G3* model and more than 40% more than the *S3* model for all three above-mentioned linear wave properties although all these three models need to solve three horizontal velocity unknowns.
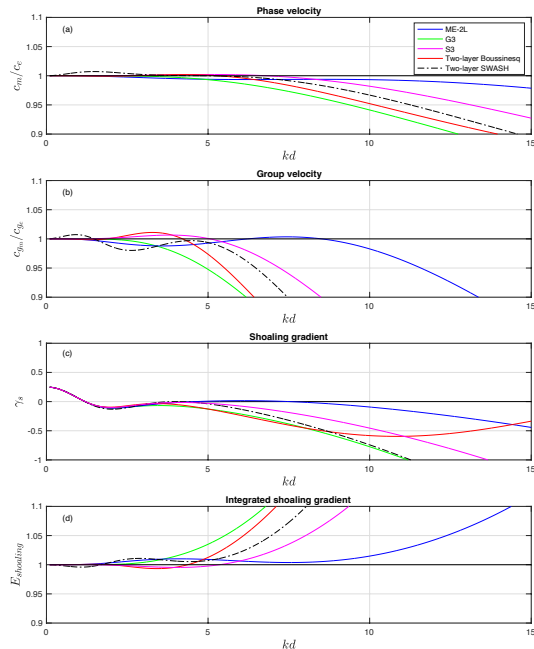

Figure 1 Comparisons of linear wave properties among *ME-2L* model, *G3* model, *S3* model, two-layer Boussinesq model and two-equidistant-layer SWASH model.

Similarly, the performance of models up to four elements in terms of various linear wave properties is summarized in figure 2, which are denoted by dash-dotted lines. It has been shown in Yang & Liu (2020) that *SK* models are superior to *GK* models, thus only *SK* models are included in the same figure for comparisons. For the multi-linear-element models, the applicable range of kd values

increase dramatically with increasing number of elements, which demonstrates the advantage of the multi-element approach in enhancing model capabilities. For models with the same number of unknowns (lines of the same color in figure 2), the multi-linear-element models outperform the *SK* models significantly. Finally, by specifying an error bound of 2% in phase velocity, while the *ME-2L* model is applicable up to $kd \approx 14.7$, *ME-4L* model significantly extends the applicable range to $kd \approx 127.9$, which is essentially in infinitely deep water.
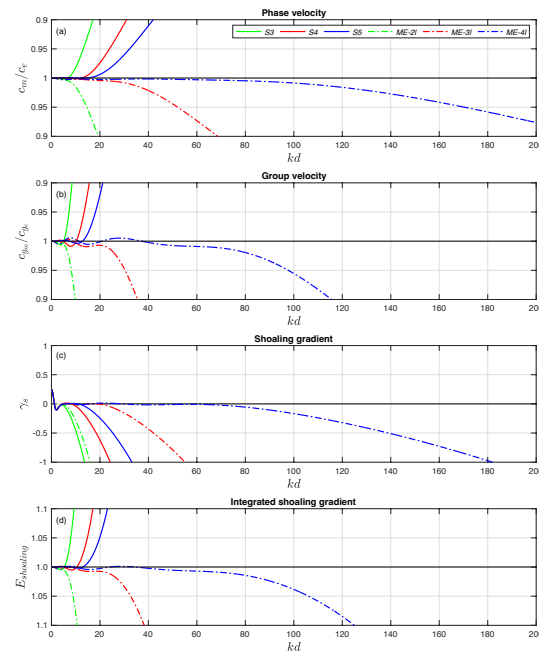

Figure 2 Comparisons of various linear wave properties between the multi-linear-element models and *SK* models (Yang & Liu 2020).

NUMERICAL VALIDATIONDS
The present *ME-2L* model is implemented numerically using the same method as discussed in Yang & Liu (2020), which employed a standard finite difference scheme for spatial discritization combined with a fourth-order Runge-Kutta method for time integration. Models of more linear elements can be implemented in the same manner as they share similar equations structures. The numerical applications of models with higher approximations, especially in very deep-water conditions, will be investigated in future studies.

The transformation of a wave train over a submerged shoal (Dingemans 1994) has been a standard test case for many depth-integrated models and fully three-dimensional models. A submerged bar with a front slope of 1/20 and a back slope of 1/10 is placed in the middle of the wave flume in a still water depth of 0.86m. Free surface elevations are measured at several wave gauges in front, on and behind the submerged bar. The incident wave has an amplitude of 0.02m and a period of 2.86s, representing a small amplitude wave propagating in a finite water depth of $kd = 0.7$. Because of the shoaling effects when waves climb on the front slope of the bar, it

becomes increasing demanding for the numerical model to accurately predict the free surface elevations behind the bar, which challenges the model's capability of not only linear wave frequency dispersion but also higher-order nonlinear effects.

Figure 3 shows the comparisons of time series of free surface elevations at eight wave gauges between the numerical results from the *ME-2L* model and experimental data. Very good agreements are found at all eight wave gauges, including the last three wave gauges, where higher harmonic waves are already in deep water conditions. It should be noted that Lin & Li (2002) used a finite difference scheme for solving the full Navier-Stokes equations in the σ-coordinate in three dimensions. Twenty meshes were used in the vertical direction for simulating the same case and the comparisons at the last three wave gauges are less satisfactory than the present model which only employs two elements in the vertical direction.

Stelling, Zijlema (2003): An accurate and efficient finite-difference algorithm for non-hydrostatic free-surface flow with application to wave propagation. International journal for numerical methods in fluids 43.1: 1-23.

Yang, Liu (2020): Depth-integrated wave-current models. Part 1. Two-dimensional formulation and applications, Journal of Fluid Mechanics, 883.
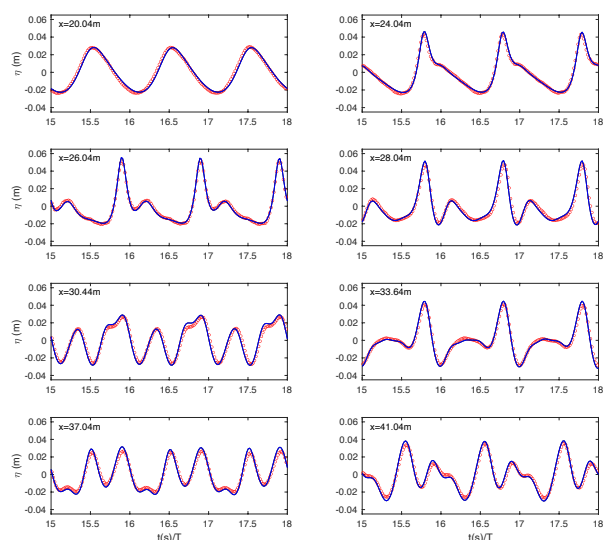
Figure 3 Comparisons between the numerical results (blue line) and experimental data (red circles) at eight wave gauges.

REFERENCES
Dingemans (1994): Comparison of computations with Boussinesq-like models and laboratory measurements. memo in framework of MAST project (G8-M), Delft Hydraulics memo H1684.12.

Lin, Li (2002): A σ-coordinate three-dimensional numerical model for surface wave propagation. International Journal for Numerical Methods in Fluids, 38(11), 1045-1068.

Lynett, Liu (2004): A two-layer approach to wave modelling. Proceedings of the Royal Society of London. Series A: Mathematical, Physical and Engineering Sciences, 460(2049), 2637-2669